Focal Benign Liver Lesions and Their Diagnostic Pitfalls

Edouard Reizine, MD, Sébastien Mulé, MD, PhD*, Alain Luciani, MD, PhD

KEYWORDS

• Liver neoplasms • Focal nodular hyperplasia • Hepatocellular adenoma • Hemangioma

KEY POINTS

- A combination of MRI features – including contrast on T1/T2WI, homogeneity, dynamic enhancement profile, lack of capsule, presence of a typical central stellate area – is required for the diagnosis of focal nodular hyperplasia. These features remain specific even in male patients or in FNH lesions containing fat. However, isolated central stellate areas or hyperintensity on hepatobiliary phase acquisitions can be observed in other lesions, including malignant lesions.
- Different subtypes of hepatocellular adenomas – including inflammatory HCA, HNF1α-inactivated HCA, and ß catenin-mutated HCA – are associated with specific MRI features including native T1IP/OP, T2, dynamic enhancement profile, and various uptake patterns on hepatobiliary phase after liver-specific contrast agent injection. Nevertheless, some other features can be misleading, mimicking focal nodular hyperplasia or malignant lesions.
- Hepatic cysts and liver hemangiomas are common incidental findings in liver MRI. However, some features, such as septations or internal heterogeneous content within a cyst, should be analyzed carefully. Moreover, some atypical hemangioma presentations can be misleading, and sometimes formal diagnosis by pathology is warranted to exclude malignant lesions.
- The specific features associated with benign liver lesions can only be assessed provided that chronic liver disease or underlying primary malignant lesions have been excluded, using clinical, biological and radiological data.

INTRODUCTION

Focal hepatic lesions are frequently discovered incidentally on cross-sectional imaging or abdominal ultrasound,[1,2] and in the general population, a vast majority of those incidental findings are benign entities.[1] However, the formal diagnosis of benign liver lesions is not always straightforward and may require advanced imaging modalities, such as MRI with hepatobiliary contrast agent or contrast-enhanced ultrasound (CEUS).[3] This review presents the typical features of the main benign liver lesions, including focal nodular hyperplasia (FNH), hepatocellular adenoma (HCA), hepatic cysts, hemangioma, angiomyolipoma, and pseudotumors, such as inflammatory pseudotumors or hepatic granulomas. However, beyond the specific and classical MRI features, some lesions may present atypical patterns. Moreover, arterial phase hyperenhancement, often present in benign liver lesions, can be seen in malignant lesions such as hepatocellular carcinoma. Hence, accurate analysis of clinical and biological contexts is mandatory to optimize our diagnostic performance. The objective of this investigation was, therefore, to review the specific

Medical Imaging, Henri Mondor University Hospital, Faculté de Médecine, Universite Paris Est, INSERM Unit U 955, Equipe 18, Creteil 94010, France
* Corresponding author.
E-mail address: sebastien.mule@aphp.fr

Radiol Clin N Am 60 (2022) 755–773
https://doi.org/10.1016/j.rcl.2022.05.005

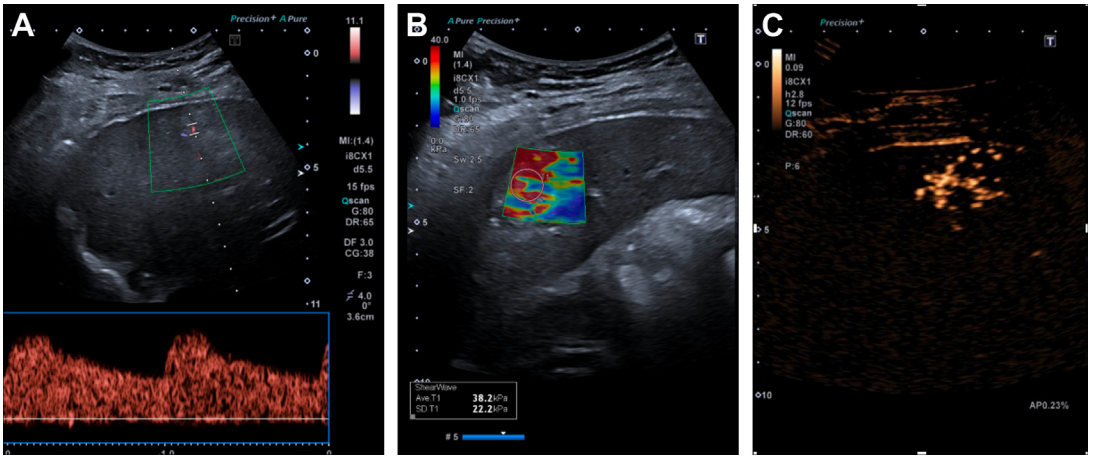

Fig. 1. Typical sonographic features of focal nodular hyperplasia. Color Doppler examination reveals the presence of a penetrating arterial vessel (*A*), and shear wave elastography shows high stiffness values (*B*). On contrast-enhanced ultrasound, after the injection of 2.4 mL of sulfur hexafluoride SonoVue, the lesion was enhanced in the arterial phase, demonstrating a typical spoke-wheel aspect with centrifugal distribution (*C*).

presentations of benign liver tumors and to illustrate their diagnostic pitfalls.

HEPATOCELLULAR LESION

Focal Nodular Hyperplasia

Focal nodular hyperplasia (FNH) is the most frequent benign hepatocellular lesion,[2] even if according to the WHO classification, FNH is not a true neoplasm but rather a mass-forming hyperplastic response of hepatocytes related to localized vascular abnormalities.[4] In 80% to 90% of cases, FNH is discovered in young women and rarely in men.[4] The background liver is usually normal, but FNH can occur in association with vascular diseases.[5,6] Usually, the lesions are incidentally found on ultrasound, where FNH shows variable nonspecific patterns of appearance on grayscale US and may sometimes only be detected because of the displacement of the surrounding vessels.[7] Typically, color Doppler examination reveals the presence of penetrating arterial vessel branching from the hepatic arterial tree directed toward the lesion. The presence of a single central artery is seen in up to 77% of FNHs, and it is not correlated with the size of the lesion.[8] Few studies have focused on shear wave elastography values for the characterization of focal liver lesions, describing high stiffness values when compared with the surrounding liver and significantly higher values than other benign lesions.[9] However, they have failed to differentiate these focal liver lesions from hepatocellular adenoma (HCA).[10]

Hence, a second imaging examination is often required to provide a formal noninvasive diagnosis. This can be achieved with contrast-enhanced ultrasound (CEUS) or MR imaging, as specific features have been associated with both techniques.[11]

With CEUS, FNH enhances at the early arterial phase (ie, 10–15 s after injection) and becomes homogeneously isoechoic after 30 s in most cases. It has been associated with two specific features:

- A spoke-wheel aspect, encountered in 20% to 25% of lesions;
- A centrifugal filling, more frequent in lesions smaller than 3 cm.[12]

A summary of typical sonographic features of FNH is presented in **Fig. 1**.

However, CEUS shows reduced sensitivity in diagnosing FNH lesions larger than 35 mm,[13,14] and MRI is usually required in that setting.

On MRI, the diagnosis of FNH is based on a combination of features, using seven major criteria to assess a proper diagnosis,[8,15,16] summarized in **Box 1** and illustrated in **Fig. 2**.

However, it is crucial to remember that an isolated feature is not sufficient for a confident diagnosis of FNH. For instance, an isolated central stellate area can be present in a wide range of liver tumors, including malignant lesions, as illustrated in **Fig. 3**.

In contrast to specificity, the sensitivity of MRI for an FNH diagnosis lags below 100%,[17–19] mainly because of the lack of a central element for lesions measuring less than 3 cm.[20] As CEUS can be misleading for lesions greater than 3.5 cm,[20] use of MRI with hepatobiliary contrast agents—i.e., gadobenate dimeglumine (Gd-BOPTA, Multihance, Bracco, Milan, Italy) or gadoxetate disodium (Gd-EOB-DTPA, Eovist or

Box 1
Major criteria on MRI for the diagnosis of focal nodular hyperplasia

- Native contrast close to that of the liver: Not different from the liver before contrast injection, that is, iso- or hypointense on T1-weighted images and iso- or slightly hyperintense on T2-weighted images
- Homogeneity apart from the central scar
- Central stellate area: Presence of a central hypointense area on T1-weighted images and strongly hyperintense on T2-weighted images
- Dynamic enhancement profile: Intense and transient enhancement in the arterial phase without washout
- No capsule
- Lobulated aspect
- Absence of underlying chronic liver disease or clinical history of cancer

Primovist, Bayer Healthcare Pharmaceuticals, Whippany, NJ, USA)—can increase the sensitivity or the diagnosis of FNH.[21] In accordance with the molecular background where FNH demonstrates increased expression of OATP,[22–24] FNH appears iso- or hyperintense on hepatobiliary-phase MRI in 94%–97% of cases,[21] with four main patterns: homogeneously hyperintense, inhomogeneously hyperintense, isointense and hypointense-with-ring.[25]

Several atypical presentations of FNH have been reported, often leading to targeted liver biopsy for final diagnosis. One common pitfall in FNH imaging is the presence of internal steatosis. Even if the presence of fat within the hepatocytes in FNH is not rare—as prior studies have found that up to 50% of FNHs contain fat on pathologic analysis[26,27]—it is less commonly seen on MRI, as only 10% of all FNHs demonstrate signal drop-out on out-of-phase imaging.[28] Although fat content can be misleading in some MRI sequences; however, it should not reduce the diagnostic confidence if all the major criteria are present,[28] as illustrated in **Fig. 4**.

More rarely, FNH can appear atypical in almost all sequences, with particularly high signal intensity on T2WI sequences and persistent enhancement in the enhanced delayed phase, suggestive of inflammatory changes, as illustrated in **Fig. 5**. Such atypical presentation is usually related to an unusually marked sinusoidal dilatation within FNH lesions.[29] This presentation should not be mistaken for inflammatory hepatocellular adenoma, and targeted liver biopsy can often be proposed in this setting if hepatobiliary phase (HBP) MRI and/or CEUS appear nonconclusive.

Finally, although FNHs are rare in men, this situation can occur, and similar to the presence of internal fat, a typical appearance on MRI should not lead to questioning the diagnosis even if particular attention to all atypical features is mandatory in that setting.[30]

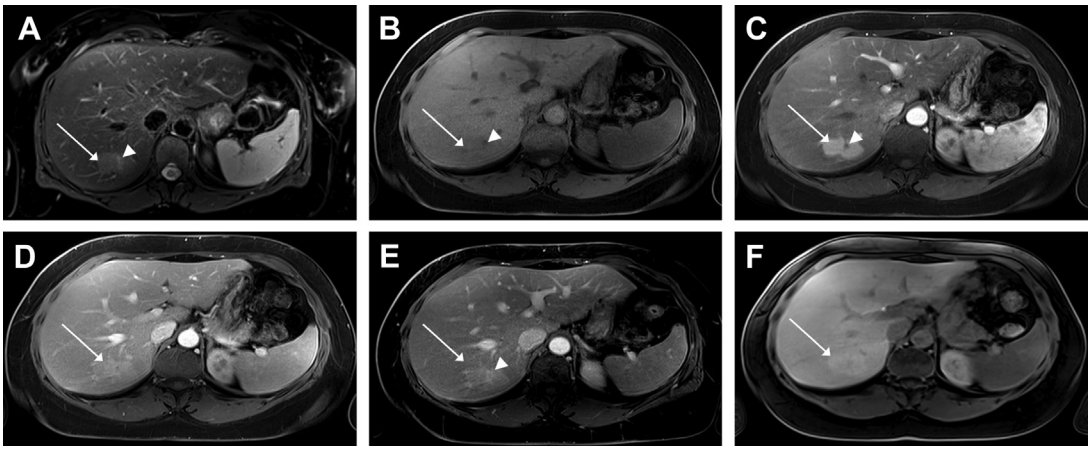

Fig. 2. Typical MRI features of FNH. Lobulated lesion, slightly hyperintense on T2-weighted fat-saturated image (*A*) and isointense on T1-weighted fat-saturated image (*B*). After injection of gadobenate dimeglumine (0.1 mL/kg), the lesion shows homogeneous arterial phase hyperenhancement (*C*) without washout in the portal venous phase (*D*) or delayed phase (*E*). There is a central element (*arrowhead*) that is hyperintense on T2-weighted fat-saturated image and hypointense on T2-weighted fat-saturated image with delayed hyperenhancement. In the hepatobiliary phase (*F*), the lesion demonstrates homogeneous hyperintensity consistent with increased uptake of the contrast agent, promoted by increased OATP expression on a molecular basis.

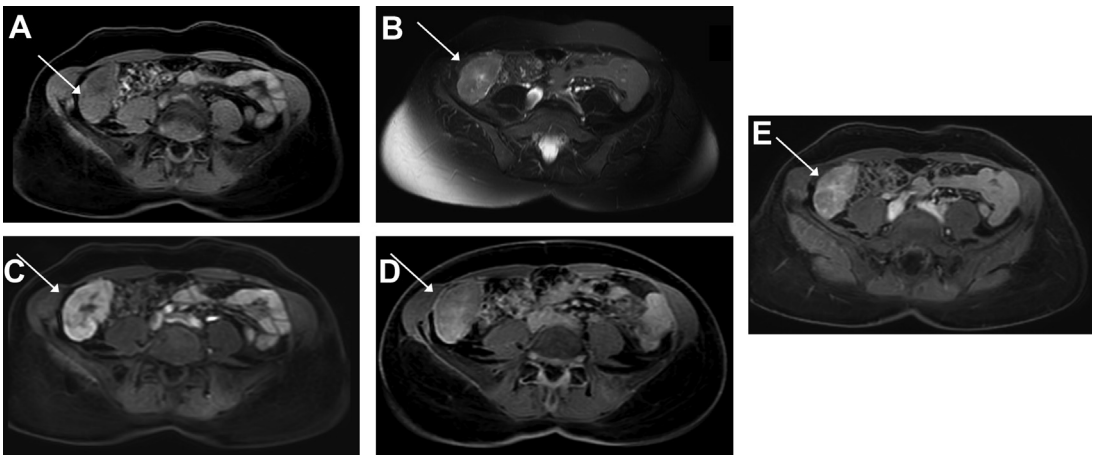

Fig. 3. Pitfall of a lesion with central element. Pedunculated lesion, hypointense on T1-weighted fat-saturated image (*A*), slightly hyperintense on T2-weighted fat-saturated image (*B*), demonstrating arterial phase hyperenhancement after injection of gadobenate dimeglumine (0.1 mL/kg) (*C*) with washout in the delayed phase (*D*), apart from delayed hyperenhancement of a central element. In the hepatobiliary phase (*E*), the lesion was hypointense with only central accumulation of gadobenate dimeglumine. The final diagnosis determined by pathology was mixed hepatocholangiocarcinoma.

HCA

Hepatocellular adenomas (HCAs) are rare benign hepatocellular tumors that mainly develop in young women.[31–33] The main risk factors are oral contraceptive use in reproductive-age women and obesity and androgen exposure in men.[34–36] The two main complications are tumor hemorrhage and malignant transformation, which can both justify liver resection in high-risk patients.[37]

A few years ago, the European Association for the Study of the Liver (EASL) issued recommendations for the management of HCA,[37] acknowledging that the risk of complications is mostly influenced by tumor size and patient sex.[38,39] Moreover, the subtyping of HCA should also be considered as different subtypes are associated with different outcomes.[34,40,41] In 2017, a new classification identified five main subgroups[34,42]:

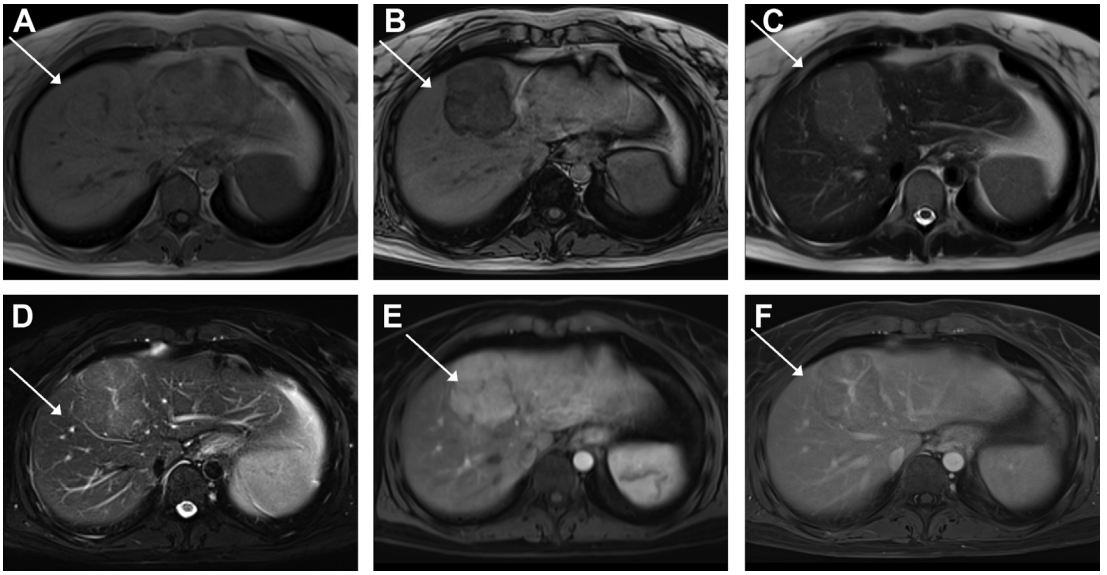

Fig. 4. Example of steatotic focal nodular hyperplasia. Lobulated lesion with homogeneous dropout of signal on the T1-opposed-phase-weighted image (A+ B), with otherwise typical features of focal nodular hyperplasia on T2-HASTE (*C*), T2-weighted fat-saturated image (*D*), arterial phase (*E*), and delayed phase (*F*).

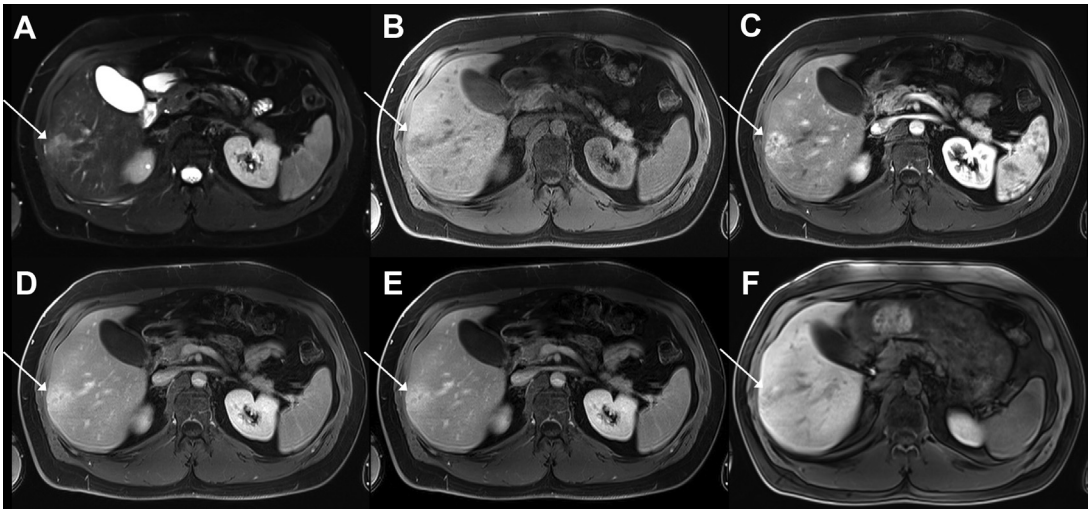

Fig. 5. Illustration of atypical FNH with sinusoidal distension. Heterogeneous lesion with irregular margins, containing area hyperintense on T2-HASTE fat-saturated image (*A*) and hypointense on T1-weighted fat-saturated image (*B*) corresponding to sinusoidal distension. The lesion showed arterial phase hyperenhancement after injection of gadobenate dimeglumine (0.1 mL/kg) (*C*), without washout in the portal venous phase (*D*) and delayed phase (*E*). The lesion exhibited peripheral uptake in the hepatobiliary phase (*F*), consistent with the final pathologic diagnosis of focal nodular hyperplasia.

- *HNF1α-inactivated HCA (HHCA)* accounts for 35%–40% of HCA and is characterized by biallelic inactivation of *hepatocyte nuclear factor 1 alpha*, thus explaining its association with maturity-onset diabetes of the young (MODY). HHCAs are usually multiple and, importantly, associated with a low risk of malignant transformation or bleeding. In pathologic analysis, HHCAs are characterized by marked steatosis, and their diagnosis is based on immunohistochemistry (IHC) to detect a downregulation of the expression of liver fatty acid-binding protein (LFABP). On MRI, a diffuse and homogeneous drop in signal intensity on out-of-phase T1-weighted MR images has a sensitivity between 87% and 91% and a specificity between 89% and 100% for the diagnosis of HHCA.[43,44] Typical HHCAs are also usually iso- or hypointense on T2-weighted images with fat suppression sequences and demonstrate faint arterial hyperenhancement.[45]
- *Inflammatory HCA (IHCA)* accounts for 35%–45% of all HCAs. IHCA is defined by activation of the IL-6/JAK/STAT pathway, leading to an inflammatory reaction. The main risk factors are estrogen exposure, obesity, alcohol use, and glycogen storage diseases. This subtype is associated with a high risk of bleeding. On IHC, there is specific overexpression of C-reactive protein (CRP) and serum amyloid A (SAA). On MRI, the combination of marked hyperintensity on T2-weighted images and persistent enhancement in the delayed phase has a sensitivity between 85% and 88% and a specificity between 88% and 100% for the diagnosis of IHCA.[43,44] In addition, IHCA tended to appear hyperintense on T1 FS-weighted imaging (WI) precontrast, particularly when associated with underlying hepatic steatosis. Moreover, given its association with obesity, internal fat is not rare in IHCA, as illustrated in **Fig. 6**, and careful analysis of the other sequences, in particular signal intensity on T2 FS WI, is crucial to avoid mistaking IHCA for HHCA.
- *β-catenin-activated HCA (BHCA)* accounts for 15%–20% of HCAs. The main risk factors are androgen exposure, liver vascular disease, and glycogen storage diseases, which explains why it is more common in men. Approximately 50% of this subtype is associated with inflammatory changes. This subtype includes different subgroups according to the type of deletion in CTNNB1. Hence, exon 3 involvement is associated with high activation of the β-catenin pathway although exon 7 and 8 involvement is linked to low activation of the β-catenin pathway. Importantly, only high activation of the β-catenin pathway is associated with a high risk of malignant transformation.[34] In IHCA, pathologic diagnosis is based on the strong homogeneous cytoplasmic expression of glutamine synthetase with

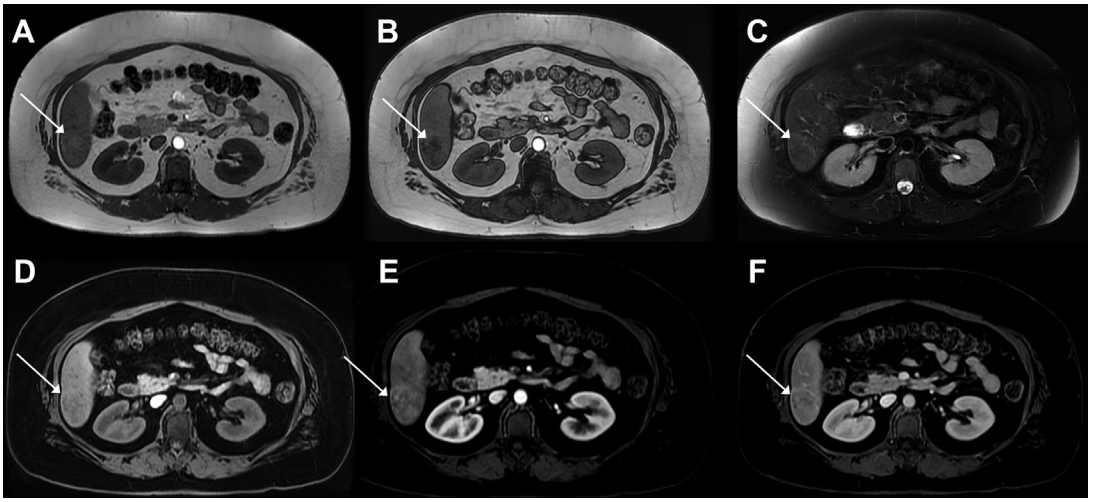

Fig. 6. IHCA-containing fat. Fat-containing lesion, with nondiffuse dropout of signal in the opposed phase (*A*, *B*), mildly hyperintense on T2-weighted fat-saturated image (*C*), isointense on T1-weighted fat-saturated image (*D*) with arterial phase hyperenhancement (*E*), and persistent enhancement in the delayed phase (*F*) consistent with the diagnosis of inflammatory adenoma.

nuclear positivity for β-catenin. However, those features are missing when the activation of β-catenin is lower (ie, involving exons 7 and 8), and screening for β-catenin mutations by molecular analysis is usually needed. Unfortunately, there are no validated imaging features for β-catenin-activated HCA to date, even though prior reports have shown that BHCA can demonstrate arterial phase hyperenhancement and wash out in the delayed phase, thus mimicking hepatocellular carcinoma.[43]

- *Sonic Hedgehog HCA (shHCA).* This recently described subtype remains rare, accounting for less than 5% of HCA. There is an important association with obesity, and there is a high risk of bleeding. Unfortunately, to date, the diagnosis of shHCA on imaging remains unclear.[40,46,47] As with BHCA, there are no specific MRI features, but a prior case report showed that shHCA could present peculiar intratumoral fluid cavities.[48]
- Finally, less than 5% of HCAs are still *unclassified* with no recognized molecular abnormality or IHC markers.

A summary of the main subtypes of HCA is provided in **Table 1**

Hence, using extracellular contrast agent, only the two main subtypes can be characterized with confidence on MRI, and a prior report showed that CEUS cannot be used in that setting.[49]

In the hepatobiliary phase on MRI, HCA typically appears hypointense, which can be useful for differentiation from FNH.[50,51] However, several recent studies have reported HCAs showing iso- or hyperintensity on HBP in up to 26% to 67% of cases,[52–54] especially following the injection of Gd-BOPTA. In most series, such iso- or hyperintensity was depicted in IHCA.[52–56] However, this is in contradiction to the molecular background of IHCA, as OATP expression has been shown to be lower than that of the adjacent liver.[24,57] Hence, HCA showing iso- or hyperintensity on the hepatobiliary phase could correspond to two different situations[58]:

- In lesions showing reduced contrast uptake on HBP, mainly IHCA, signal hyperintensity on HBP is not due to contrast uptake but to pre-existing signal hyperintensity on precontrast images and underlying hepatic steatosis, illustrated in **Fig. 7**.
- In lesions with true contrast uptake, specifically associated with marked activation of the ß-catenin pathway,[59] which is consistent with the molecular background, prior studies have shown that OATP expression is persistent in BHCA,[24,60] as illustrated in **Fig. 8**.

Hence, HBP uptake does not always correspond to FNH but could also correspond to BHCA. Moreover, diagnosis can be challenging, as both usually develop in young patients, and both can demonstrate a central element on MRI,[61] as illustrated in **Fig. 9**.

Moreover, in addition to benign hepatocellular lesions, HBP uptake should always be analyzed carefully, and differentiated hepatocellular carcinoma or nonhepatocellular lesions with fibrotic stoma can demonstrate hyperintensity on HBP.[62]

Table 1
Summary of the main subtypes of HCA

Subtypes	HNF1α-Inactivated HCA	Inflammatory HCA	β-Catenin-activated HCA		Sonic Hedgehog HCA	Unclassified
Frequency	35%–40%	35%–45%	15%–20%		5%	<5%
Risk factors	HNF1α germline	Obesity Alcohol use Glycogen storage disease	Androgen Liver vascular disease glycogen storage disease		Obesity	
Specific staining on IHC	LFABP-	CRP++ SAA++	GS +++ β-catenin +	GS+	PTGDS + ASS1+	
Main complications		Hemorrhage	High risk of malignant transformation		Hemorrhage	
Specific MRI features	Diffuse and homogeneous drop of signal on opposed phase	Marked hyperintensity on T2 and persistent enhancement on delayed phase	No specific imaging feature associated with an uptake on the hepatobiliary phase	No specific imaging feature	No specific imaging feature	

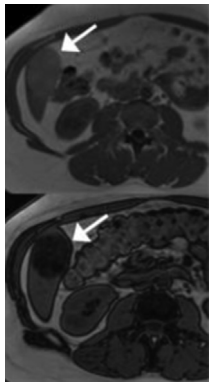

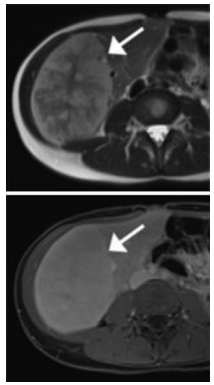

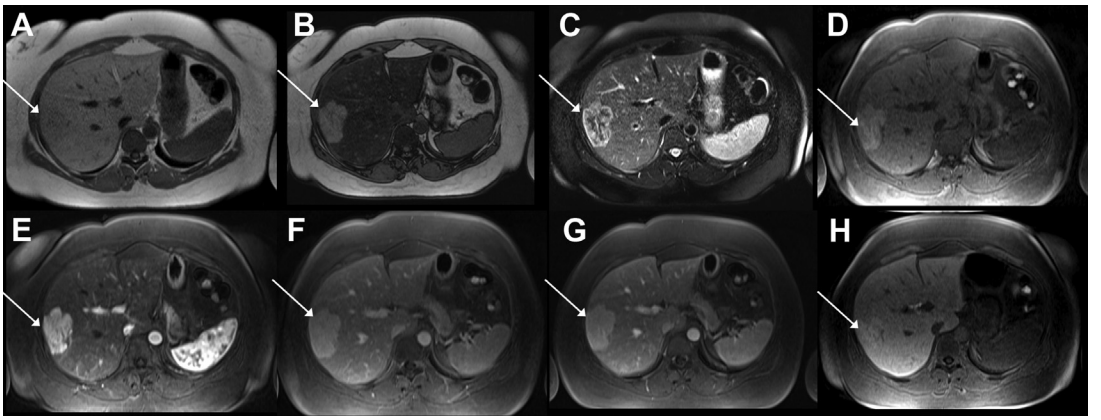

Fig. 7. Illustration of inflammatory adenoma hyperintensity in the hepatobiliary phase. Marked hepatic steatosis with homogeneous dropout of signal on the opposed-phase-weighted image (*A*, *B*), with hyperintense lesion on T2-weighted fat-saturated image (*C*), hyperintense on T1-weighted fat-saturated image (*D*), with marked arterial hyperenhancement after injection of gadobenate dimeglumine (0.1 mL/kg) (*E*) and persistent enhancement on the portal venous phase (*F*) and delayed phase (*G*). The hyperintensity on the hepatobiliary phase (*H*) seen here was related to pseudouptake in the lesion that was intrinsically hyperintense compared with the surrounding liver parenchyma due to diffuse hepatic steatosis.

There is no clear added value of metabolic imaging in HCA evaluation; however, an important pitfall is the usual avidity of HHCA on 18F-FDG PET/CT, as shown in **Fig. 10**, more so than the other HCA subtypes,[63] which mimics metastasis[64] on metabolic imaging, in particular given that this subtype is commonly associated with adenomatosis.[65]

NONHEPATOCELLULAR LESIONS

Hepatic Cysts

Hepatic cysts are the most prevalent liver lesions in the general population and can be found in 5%–18% of the general population.[66,67] On US, the characteristic imaging features are a round and completely anechoic structure, with

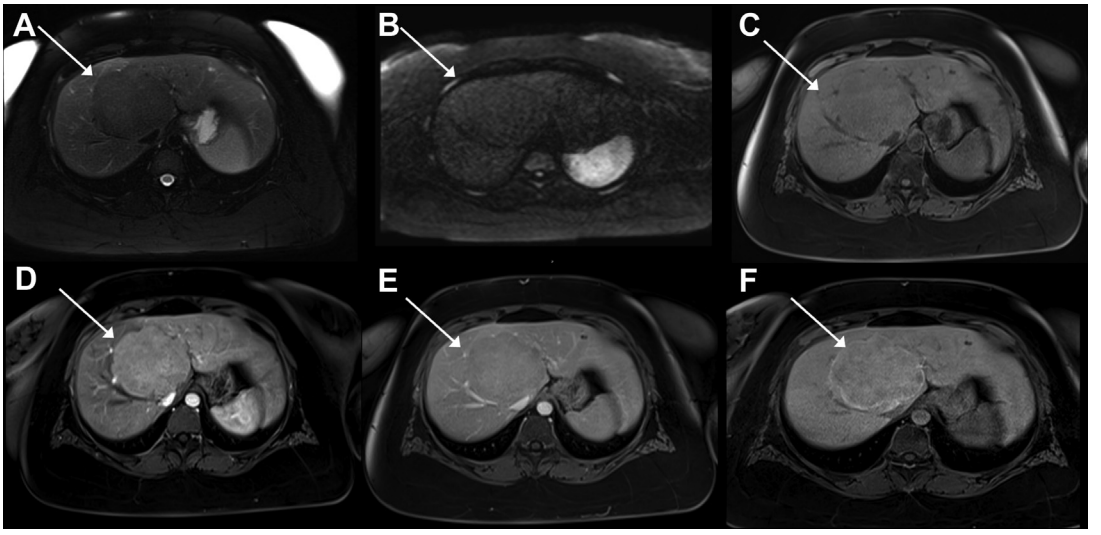

Fig. 8. β-Catenin-activated adenoma hyperintensity in the hepatobiliary phase. Large lesion hypointense on fat-saturated T2-weighted fat saturated image (*A*), without diffusion restriction (*B*), isointense on T1-weighted fat-saturated image (*C*), with arterial hyperenhancement after injection of gadobenate dimeglumine (0.1 mL/kg) (*D*) and no washout in the delayed phase (*E*). In the hepatobiliary phase (*F*), the lesion demonstrated hyperintensity consistent with a true increased uptake of gadobenate dimeglumine (0.1 mL/kg).

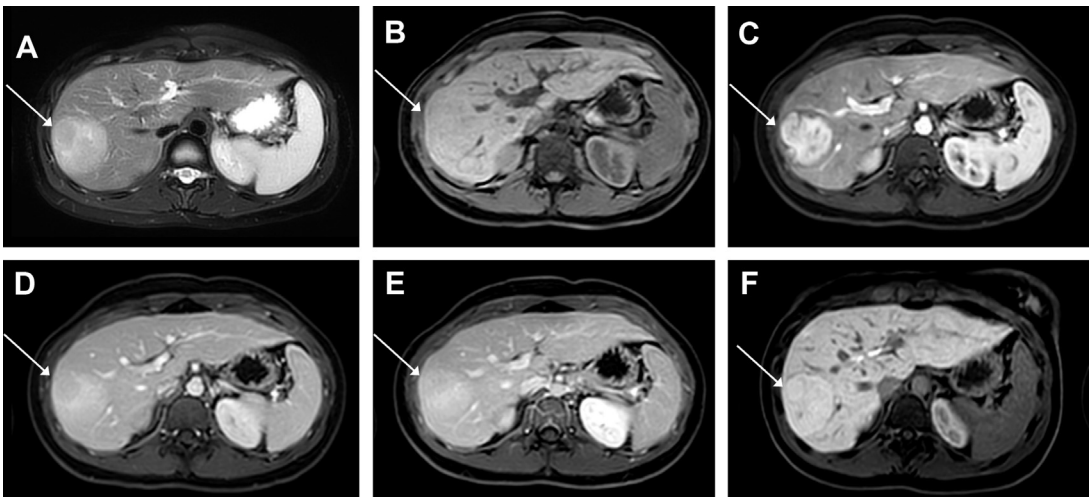

Fig. 9. Pitfall of lesion with central element hyperintensity in the hepatobiliary phase. Focal lesion slightly hyperintense on T2-weighted fat-saturated image (*A*), Isointense on T1-weighted fat-saturated image (*B*), demonstrating arterial hyperenhancement after injection of gadobenate dimeglumine (0.1 mL/kg) (*C*) without washout in the portal venous (*D*) or delayed phase (*E*) with homogeneous uptake in the hepatobiliary phase (*F*). T2 hyperintensity and minimally heterogeneous enhancement in the arterial phase were not typical for focal nodular hyperplasia. The final diagnosis made through pathology was an inflammatory β-catenin-mutated adenoma.

circumscribed margins, posterior acoustic enhancement, and no internal nodularity on color Doppler interrogation. On CT, cysts are homogeneous fluid attenuation structures, with sharp margins and no internal or mural enhancement. On MRI, they are homogenously markedly hyperintense on T2-weighted sequences, like urine, bile, and cerebrospinal fluid, with low signal on T1-weighted imaging and without any enhancement or restricted diffusion. Differential diagnosis mainly includes biliary hamartomas or von Meyenburg complexes, which are benign developmental lesions, usually multiple and measuring less than 15 mm in diameter.[68]

Rarely, hepatic cysts can demonstrate complications such as hemorrhage.[69] In those situations, differential diagnosis between a hepatic cyst and a ciliated hepatic foregut cyst (CHFC) can be troublesome.[70] CHFC is a rare solitary benign hepatic cyst appearing histologically similar to bronchogenic and esophageal duplication cysts. The majority of CHFCs are incidentally found either on imaging or intraoperatively.[71] Typically, a CHFC is a solitary lesion measuring less than 3 cm and

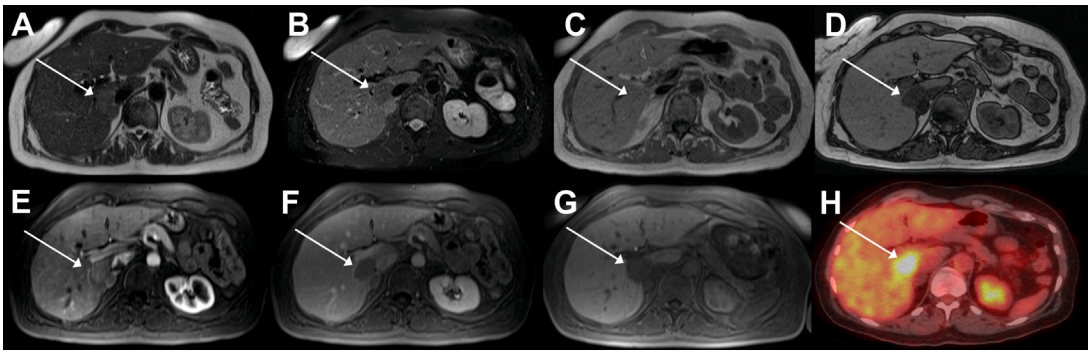

Fig. 10. HNF1α-inactivated HCA with hypermetabolism on 18F-FDG PET/CT. Typical HNF1α-inactivated HCA, slightly hyperintense on T2 HASTE (*A*) but hypointense on T2-weighted fat-saturated image (*B*), related to the diffuse and homogeneous fat content on the lesion as demonstrated by signal dropout in the T1-opposed-phase-weighted image (*C*, *D*). On postcontrast sequences after injection of gadobenate dimeglumine (0.1 mL/kg), the lesion demonstrated faint arterial hyperenhancement (*E*), with hypointensity in the delayed phase (*F*) and in the hepatobiliary phase (*G*). This lesion demonstrated marked hypermetabolism on 18F-FDG PET/CT (*H*).

is most commonly located in the subcapsular aspect of segment IV.[71] Diagnosis may be difficult on CT, as the fluid may be of greater density than simple fluid.[72,73] On MRI, signal intensity on T1-weighted images is also variable, ranging from hypointense to hyperintense,[74–76] and rarely, they may be associated with a fluid–fluid level.[77] Even if preoperative diagnosis may be difficult, CHFC recognition is crucial given that surgical management should be considered for all CHFCs.[71]

In addition to infectious lesions, one major differential diagnosis of liver cysts is mucinous cystic neoplasms, accounting for approximately 5% of all hepatic cystic lesions.[78] The previous terms "biliary cystadenoma" and "cystadenocarcinoma" should no longer be used, and according to the WHO classification, those tumors should be classified either as biliary mucinous cystic neoplasms (MCNs) of the liver and bile ducts (noninvasive for biliary cystadenoma and invasive for biliary cystadenocarcinoma) when ovarian-type stroma is present or as intraductal papillary neoplasms of the liver and bile duct (IPNB) when there is communication with bile ducts.[4] MCNs occur most commonly in Caucasian, middle-aged women.[79] A prior study found that the presence of upstream bile duct dilatation, perilesional perfusional changes, location in the left lobe, and the coexistence of fewer than three other cysts can help differentiate biliary cystic neoplasms from simple hepatic cysts.[80] In addition, a recent study found that the features most predictive of MCNs rather than simple cysts were thick septations, internal nodularity, or solid enhancing components, with advantages of MRI over CT for the detection of upstream biliary dilatation, thin septation, and internal hemorrhage or debris.[79]

Hemangioma

Hepatic hemangiomas are the most common solid benign tumors of the liver, with a prevalence between 1% and 20%.[81,82] They are frequently discovered incidentally, as most patients with hemangioma are asymptomatic and require no treatment.[82] There is a female predilection (ratio of 5:1),[82] and multiple hemangiomas may be present in 9%–22% of patients.

On ultrasound, the most common appearance consists of a homogeneous hyperechoic nodule, with discrete posterior acoustic enhancement, and without signal on Doppler evaluation.[83] On CEUS, there is peripheral discontinuous globular enhancement in the arterial phase with centripetal filling in the portal and late phases.[84] Hence, a combination of peripheral nodular arterial enhancement and complete portal venous fill-in may have 98% sensitivity for the diagnosis of hemangioma.[85]

CT features usually include a hypodense well-defined lesion, with an internal density similar to that of the vessels. After injection, slow nodular discontinuous peripheral and centripetal enhancement is observed, with typically persistent filling in the delayed phase. However, delayed complete contrast filling should not always be expected, especially for large tumors. MRI has been shown to be the best imaging modality for diagnosing hepatic hemangiomas with high sensitivity and specificity.[86] In addition to similar enhancement as described above, typical hemangiomas are hypointense on T1-weighted MR images and markedly hyperintense on T2-weighted images. On diffusion, hepatic hemangiomas typically show suppression of high signal intensity at high b values; however, a significant rate of otherwise typical hemangiomas may demonstrate residual high signal intensity on high b-value images related to the T2 shine-through effect.[86]

There are several forms of atypical hemangiomas,[81,87,88] some of which are well known and usually have a straightforward diagnosis, such as rapidly filling hemangioma, characterized by immediate homogenous enhancement in the arterial phase of contrast administration with persistent enhancement in later phases of contrast administration on CT and MR. Perilesional hepatic parenchymal transient hyperenhancement in the arterial phase is commonly associated with these hemangiomas,[89] as illustrated in **Fig. 11**.

Another classic form of atypical hemangioma is a large hemangioma, defined as giant hemangioma when the size exceeds 4 cm,[87] even if some suggest reserving the term "giant" for hemangiomas larger than 10 cm.[90] They are characterized by heterogeneous but high hyperintensity on T2, associated with areas of different T2 intensities with internal septation.[81,87,88] The enhancement kinetics are slow but identical to those of typical hemangiomas, apart from incomplete filling of the delayed phase. An example of a giant hemangioma is shown in **Fig. 12**.

In contrast, features of sclerosed hemangioma can be misleading. On pathology, there is a difference between true sclerosed hemangiomas, characterized by extensive fibrosis with marked narrowing or obliteration of the vascular spaces, and sclerosing cavernous hemangiomas, characterized by variably sized cavernous spaces lined with flattened endothelial cells with varying degrees of stromal sclerosis.[91] However, both forms usually demonstrate atypical features, in particular slight hyperintensity on T2WI with capsular retraction and calcification.[92] After injection, most

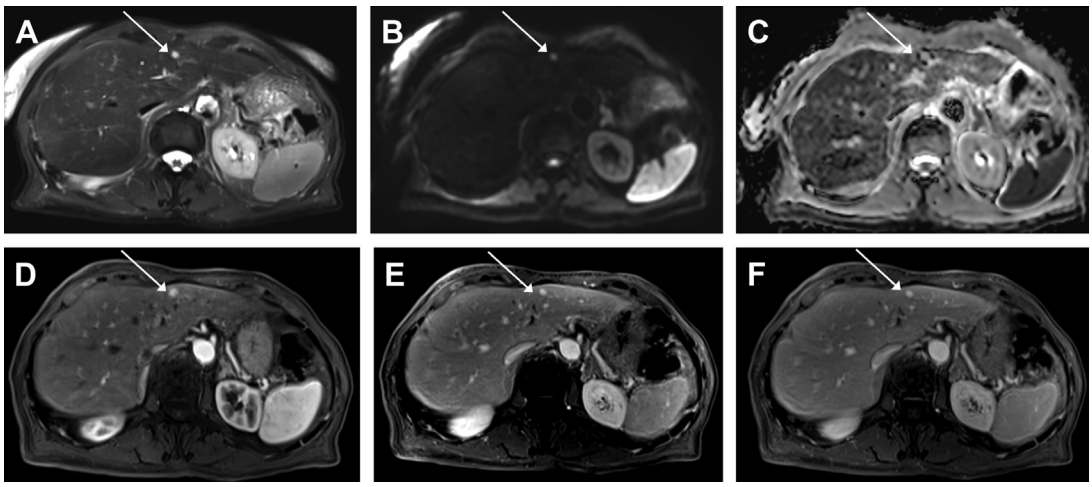

Fig. 11. Rapidly filling hemangioma. As a typical hemangioma, the lesion demonstrated marked hyperintensity on T2-weighted fat-saturated images (*A*), with slight hyperintensity on diffusion (*B*) without restriction (*C*). On the postcontrast sequences, enhancement was similar to that of the aorta in the arterial (*D*), portal venous (*E*), and delayed (*F*) phases, with perilesional transient hyperenhancement in the arterial phase.

sclerosing cavernous hemangiomas tend to demonstrate centripetal enhancement characteristics, in contrast to sclerosed hemangiomas, which usually exhibit little or no enhancement during the arterial phase and only marginal enhancement during the delayed phase.[92] Most of the time, sclerosed hemangiomas do not demonstrate diffusion restriction, which can help to differentiate them from malignant lesions,[93] as illustrated in **Fig. 13**.

Calcifications may occur in 20% of hemangiomas and are usually large and coarse and located centrally.[94] Rarely, calcifications may occur in almost all the lesions, as illustrated in **Fig. 14**.

Rare Tumors and Pseudotumors

Hepatic angiomyolipoma (HAML) is a rare mesenchymal tumor with marked female predominance and peak incidence in middle-aged adults.[4,95–97] Most of them are sporadic, and 5% to 10% of patients have tuberous sclerosis.[98]

In general, HAML is suggested when its fatty component is identified on imaging[99]; however, in addition to hepatocellular tumors that can also

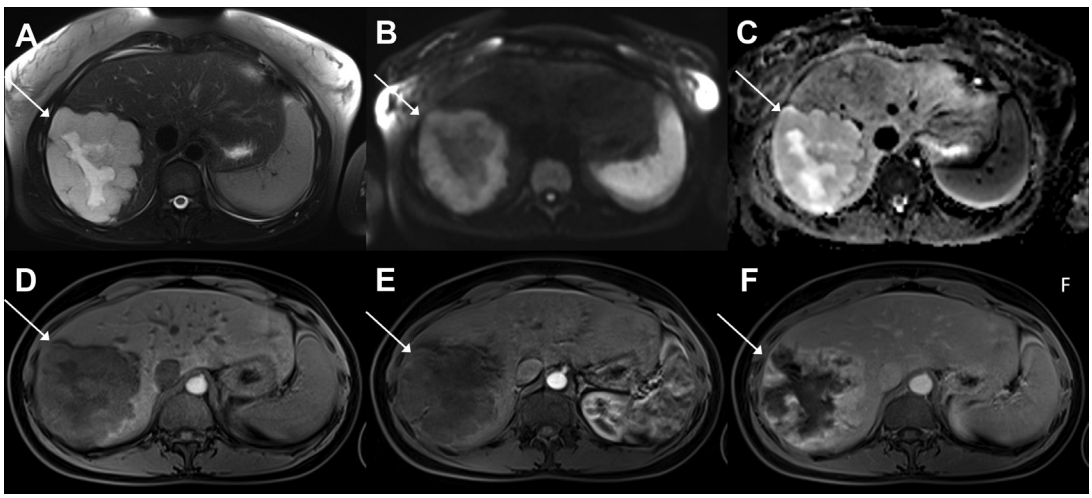

Fig. 12. Giant hemangioma. Large liver lesion with heterogeneous hyperintensity on T2-weighted fat-saturated image (*A*), hyperintensity on diffusion (*B*) without restriction (*C*). The lesion was hypointense on T1-weighted fat-saturated image (*D*) with almost no enhancement in the arterial phase I and incomplete filling in the delayed phase (*F*).

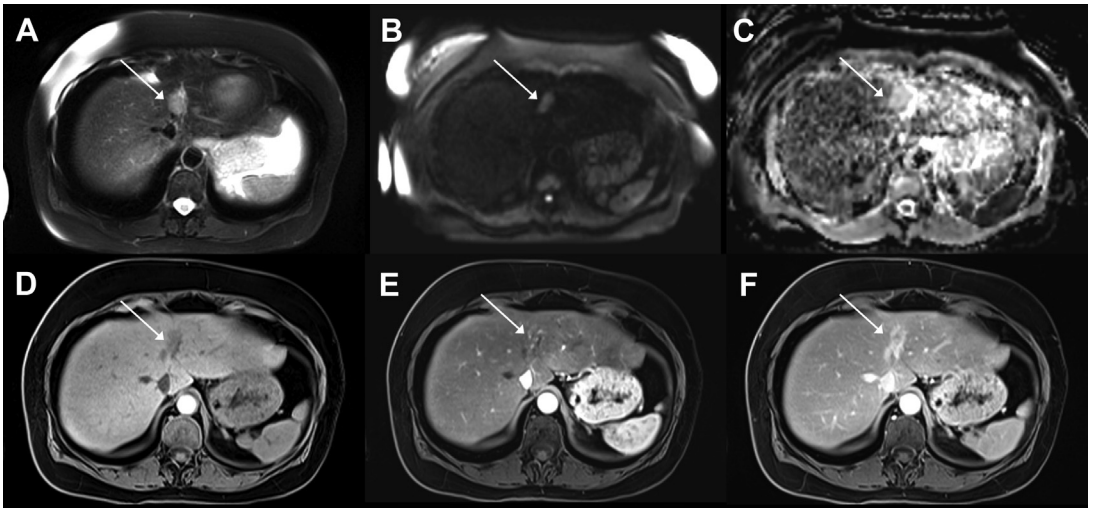

Fig. 13. Pitfalls of sclerosed hemangioma. Lesion with faint hyperintensity on fat-saturated T2-weighted image (*A*), hyperintensity on diffusion (*B*) without restriction (*C*), hypointensity on fat-saturated T1-weighted image (*D*) with faint peripheral hyperenhancement in the arterial phal(*E*) and heterogeneous rim hyperenhancement in the delayed phase (*F*). Despite the reassuring lack of diffusion restriction, a biopsy was performed to exclude fibrotic malignant lesions, and the diagnosis of sclerosed hemangioma was confirmed.

have a fat component, as seen previously, the fat content of HAML can also vary, or events sometimes cannot be recognized on MRI.[97] After contrast media injection, HAMLs demonstrate arterial hyperenhancement with typical washout on portal venous and delayed imaging,[100,101] thus mimicking hepatocellular carcinoma. In those situations, CEUS could be useful, as HAML may demonstrate specific findings such as a centripetal filling pattern or a prolonged enhancement pattern with a higher peak intensity.[102] A formal diagnosis is provided by pathology. An example of HAML is provided in **Fig. 15**.

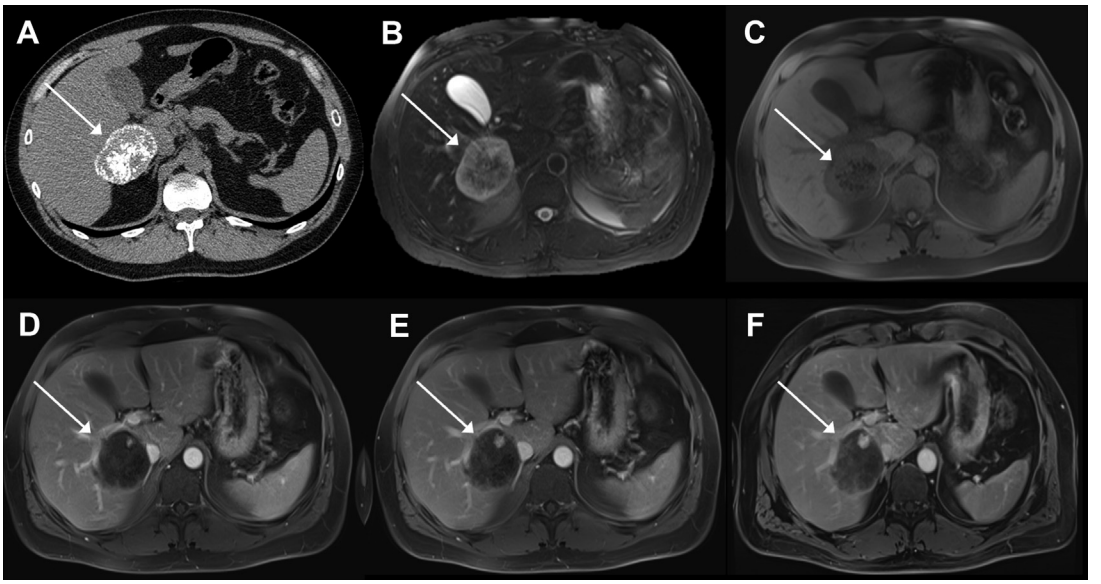

Fig. 14. Calcified hemangioma. The enhanced CT scan (*A*) showed an almost completely calcified lesion. Given the calcification, the lesion showed a heterogeneous signal intensity on fat-saturated T2-weighted imaging (*B*) and fat-saturated T1-weighted imaging (*C*). After injection of contrast, the single nodular peripheral discontinuous hyperenhancement (*D–F*) was consistent with the diagnosis of calcified hemangioma.

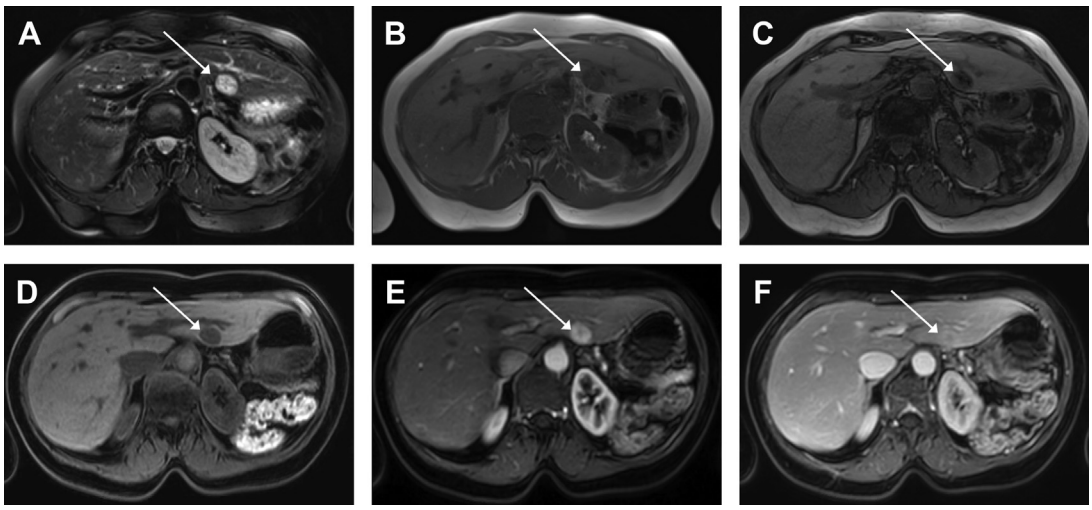

Fig. 15. Example of hepatic angiomyolipoma. Rounded lesion demonstrating faint hyperintensity on fat-suppressed T2-weighted image (*A*), with dropout of signal in the opposed phase (*B*, *C*) in keeping with the internal fat. The lesion was hypointense on fat-suppressed T1-weighted imaging (*D*), with marked arterial hyperenhancement after injection of gadobenate dimeglumine (0.1 mIg) (*E*) and no washout in the delayed phase (*F*). The diagnosis of hepatic angiomyolipoma was confirmed through biopsy.

Granulomatous hepatitis, defined as an inflammatory liver disease with the formation of granulomas in the liver, is associated with a large variety of conditions, most commonly with sarcoidosis, tuberculosis, and histoplasmosis.[103,104] According to prior reports, hepatic granulomas are present in 2.4%–10% of liver tissue specimens examined.[105,106] There is no specific imaging pattern for hepatic granulomas; however, they are often associated with diffusion restriction[107] and can mimic liver metastases,[108] as shown in **Fig. 16**.

Inflammatory pseudotumor (IPT) of the liver is a rare benign neoplasm that was first described in 1953[109] and is histologically characterized by fibroblastic and myofibroblastic proliferation with inflammatory infiltrate.[110] IPTs are now classified into two types based on IgG4 staining: IgG4-related and non-IgG4-related.[111] Usually, IPT will regress spontaneously or with conservative

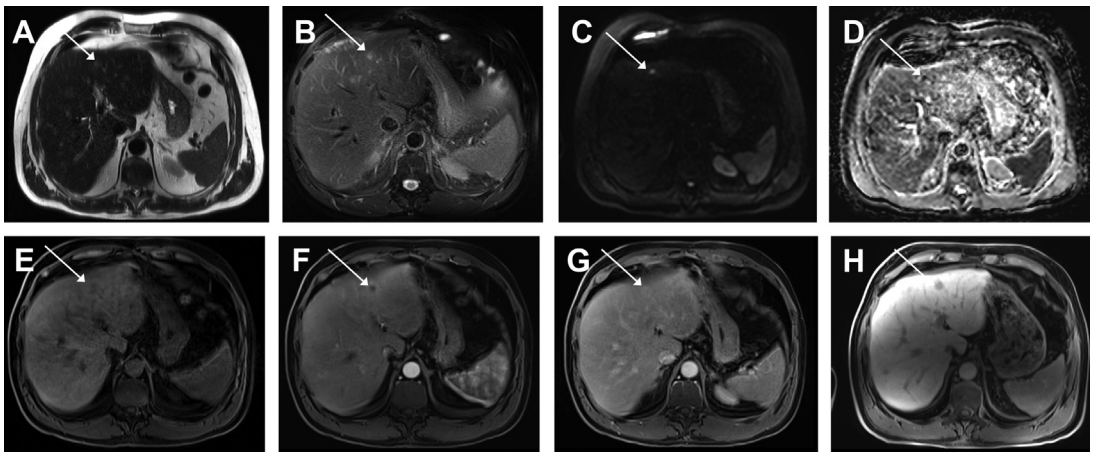

Fig. 16. Hepatic granuloma mimicking metastasis. Tiny lesion, hyperintense on T2 HASTE (*A*), better appreciated on fat-saturated T2-weighted images (*B*), hyperintense on diffusion (*C*) with restriction (*D*), hypointense on fat-saturated T1-weightelmages (*E*), with rim hyperenhancement in the arterial phase (*F*), progressive peripheral filling in the delayed phase (*G*) and no uptake in the hepatobiliary phase (*H*). Given that the patient had several similar lesions within the liver, it was mistaken for metastasis, with a final diagnosis of hepatic granuloma based on the pathologic findings.

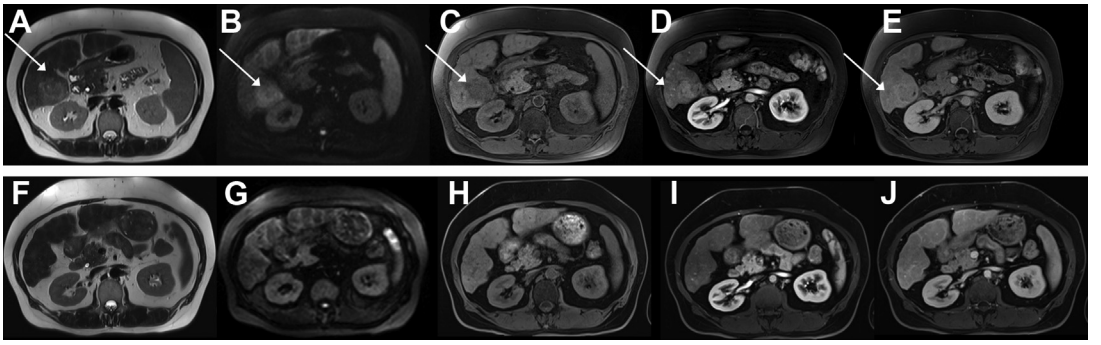

Fig. 17. Illustration of an inflammatory pseudotumor. Large lesion developed on a cirrhotic liver, hyperintense on T2 HASTE (*A*), hyperintense on diffusion (*B*), hypointense on T1 fat-suppressed WI (*C*) with arterial hyperenhancement (*D*) and no washout in the deled phase (*E*). The pathologic result was in favor of an inflammatory pseudotumor. Follow-up 3 months later showed complete resolution of the tumor on T2-weighted images (*F*), diffusion (*G*), T1 (*H*), arterial (*I*), and delayed phases (*J*).

treatment.[112] Rarely, IPT can also cause complications such as portal thrombophlebitis, portal hypertension, and biliary obstruction.[113,114] On ultrasound images, these lesions usually appear as hypoechoic masses but may also show hyperechogenicity or complex echogenicity.[115,116] On CEUS, IPTs may also display various enhancement patterns.[116] On MRI, imaging features are usually nonspecific, mostly T1 hypointense and moderately T2 hyperintense with a highly variable enhancement pattern,[117] which was the case for the example provided in **Fig. 17**. A recent study showed that IPTs may demonstrate central hypointensity with a relatively hyperintense periphery on HBP, which could be helpful to differentiate IPT from malignant lesions such as metastases.[118]

One rare differential of IPT is the inflammatory myofibroblastic tumor, a rare benign tumor, possibly representing the neoplastic counterpart of IPT,[110] characterized by fibroblastic or myofibroblastic spindle cells, admixed with lymphocytes and plasma cells, and ALK gene translocation, resulting in aberrant expression of ALK protein in the myofibroblast.[110] IMTs usually occur in children and young adults. On MRI, IMTs may show early target appearance on unenhanced T1WI, characterized by a central isointensity and a peripheral hypointense rim on unenhanced T1WI, and on early dynamic phases of gadoxetic acid-enhanced MRI, characterized by central enhancement and a peripheral hypointense rim in the arterial and portal venous phases.[119]

SUMMARY

Benign focal liver lesions include numerous tumors ranging from common incidental findings with no specific management to rare tumors with potential malignant transformation. Moreover, benign lesions can be mistaken for malignant lesions. Hence, optimal instrumentation using MRI, often performed using a hepatobiliary contrast agent, and contrast-enhanced ultrasound is the cornerstone for optimized diagnostic pathways. Multidisciplinary tumor boards, bringing together hepatologists, pathologists, radiologists, and surgeons, should address difficult cases of benign liver tumors to allow improved patient management.

CLINICS CARE POINTS

- Optimal instrumentation using MRI, often performed using a hepatobiliary contrast agent, and contrast-enhanced ultrasound are the cornerstone for optimized diagnosis in benign liver lesions.
- Typical Focal Nodular Hyperplasia and main Hepatocellular Adenoma subtypes can be characterized on MRI, however carefull analysis of MRI features is mandatory to avoid potential pitfalls.
- Hepatic cysts and liver hemangiomas are common incidental findings in liver MRI. However, some features, such as septations or internal heterogeneous content within a cyst, should be analyzed carefully.

DISCLOSURE

The authors have nothing to disclose.

REFERENCES

1. Gore RM, Pickhardt PJ, Mortele KJ, et al. Management of Incidental Liver Lesions on CT: A White Paper of the ACR Incidental Findings Committee. J Am Coll Radiol 2017;14(11):1429–37.
2. Kaltenbach TE-M, Engler P, Kratzer W, et al. Prevalence of benign focal liver lesions: ultrasound investigation of 45,319 hospital patients. Abdom Radiol 2016;41:25–32.
3. Nault J-C, Blanc J-F, Moga L, et al. Non-invasive diagnosis and follow-up of benign liver tumours. Clin Res Hepatol Gastroenterol 2021;101765. https://doi.org/10.1016/j.clinre.2021.101765.
4. Nagtegaal ID, Odze RD, Klimstra D, et al. The 2019 WHO classification of tumours of the digestive system. Histopathology 2020;76(2):182–8.
5. Sempoux C, Balabaud C, Paradis V, et al. Hepatocellular nodules in vascular liver diseases. Virchows Arch Int J Pathol 2018;473(1):33–44.
6. Vilgrain V, Paradis V, Van Wettere M, et al. Benign and malignant hepatocellular lesions in patients with vascular liver diseases. Abdom Radiol N Y 2018;43(8):1968–77.
7. Bartolotta TV, Midiri M, Scialpi M, et al. Focal nodular hyperplasia in normal and fatty liver: a qualitative and quantitative evaluation with contrast-enhanced ultrasound. Eur Radiol 2004; 14(4):583–91.
8. Ronot M, Vilgrain V. Imaging of benign hepatocellular lesions: current concepts and recent updates. Clin Res Hepatol Gastroenterol 2014;38(6):681–8.
9. Ronot M, Di Renzo S, Gregoli B, et al. Characterization of fortuitously discovered focal liver lesions: additional information provided by shearwave elastography. Eur Radiol 2015;25(2):346–58.
10. Taimr P, Klompenhouwer AJ, Thomeer MGJ, et al. Can point shear wave elastography differentiate focal nodular hyperplasia from hepatocellular adenoma. J Clin Ultrasound 2018;46(6):380–5.
11. Soussan M, Aubé C, Bahrami S, et al. Incidental focal solid liver lesions: diagnostic performance of contrast-enhanced ultrasound and MR imaging. Eur Radiol 2010;20(7):1715–25.
12. Wang W, Chen L-D, Lu M-D, et al. Contrast-enhanced ultrasound features of histologically proven focal nodular hyperplasia: diagnostic performance compared with contrast-enhanced CT. Eur Radiol 2013;23(9):2546–54.
13. Roche V, Pigneur F, Tselikas L, et al. Differentiation of focal nodular hyperplasia from hepatocellular adenomas with low-mechanical-index contrast-enhanced sonography (CEUS): effect of size on diagnostic confidence. Eur Radiol 2015;25(1):186–95.
14. Bertin C, Egels S, Wagner M, et al. Contrast-enhanced ultrasound of focal nodular hyperplasia: a matter of size. Eur Radiol 2014;24(10):2561–71.
15. Mathieu D, Rahmouni A, Anglade MC, et al. Focal nodular hyperplasia of the liver: assessment with contrast-enhanced TurboFLASH MR imaging. Radiology 1991;180(1):25–30.
16. Dioguardi Burgio M, Ronot M, Salvaggio G, et al. Imaging of Hepatic Focal Nodular Hyperplasia: Pictorial Review and Diagnostic Strategy. Semin Ultrasound CT MR 2016;37(6):511–24.
17. Bieze M, van den Esschert JW, Nio CY, et al. Diagnostic accuracy of MRI in differentiating hepatocellular adenoma from focal nodular hyperplasia: prospective study of the additional value of gadoxetate disodium. AJR Am J Roentgenol 2012;199(1): 26–34.
18. Ferlicot S, Kobeiter H, Tran Van Nhieu J, et al. MRI of atypical focal nodular hyperplasia of the liver: radiology-pathology correlation. AJR Am J Roentgenol 2004;182(5):1227–31.
19. Grazioli L, Morana G, Federle MP, et al. Focal nodular hyperplasia: morphologic and functional information from MR imaging with gadobenate dimeglumine. Radiology 2001;221(3):731–9.
20. Tselikas L, Pigneur F, Roux M, et al. Impact of hepatobiliary phase liver MRI versus Contrast-Enhanced Ultrasound after an inconclusive extracellular gadolinium-based contrast-enhanced MRI for the diagnosis of benign hepatocellular tumors. Abdom Radiol N Y 2017;42(3):825–32.
21. Suh CH, Kim KW, Kim GY, et al. The diagnostic value of Gd-EOB-DTPA-MRI for the diagnosis of focal nodular hyperplasia: a systematic review and meta-analysis. Eur Radiol 2015;25(4):950–60.
22. Yoneda N, Matsui O, Kitao A, et al. Hepatocyte transporter expression in FNH and FNH-like nodule: correlation with signal intensity on gadoxetic acid enhanced magnetic resonance images. Jpn J Radiol 2012;30(6):499–508.
23. Fujiwara H, Sekine S, Onaya H, et al. Ring-like enhancement of focal nodular hyperplasia with hepatobiliary-phase Gd-EOB-DTPA-enhanced magnetic resonance imaging: radiological-pathological correlation. Jpn J Radiol 2011; 29(10):739–43.
24. Reizine E, Amaddeo G, Pigneur F, et al. Quantitative correlation between uptake of Gd-BOPTA on hepatobiliary phase and tumor molecular features in patients with benign hepatocellular lesions. Eur Radiol 2018. https://doi.org/10.1007/s00330-018-5438-7.
25. van Kessel CS, de Boer E, ten Kate FJW, et al. Focal nodular hyperplasia: hepatobiliary enhancement patterns on gadoxetic-acid contrast-enhanced MRI. Abdom Imaging 2013;38(3): 490–501.
26. Nguyen BN, Fléjou JF, Terris B, et al. Focal nodular hyperplasia of the liver: a comprehensive pathologic study of 305 lesions and recognition of new

histologic forms. Am J Surg Pathol 1999;23(12):1441–54.
27. Hussain SM, Semelka RC, Mitchell DG. MR imaging of hepatocellular carcinoma. Magn Reson Imaging Clin N Am 2002;10(1):31–52, v.
28. Ronot M, Paradis V, Duran R, et al. MR findings of steatotic focal nodular hyperplasia and comparison with other fatty tumours. Eur Radiol 2013;23(4):914–23.
29. Laumonier H, Frulio N, Laurent C, et al. Focal nodular hyperplasia with major sinusoidal dilatation: a misleading entity. BMJ Case Rep 2010;2010. bcr0920103311.
30. Luciani A, Kobeiter H, Maison P, et al. Focal nodular hyperplasia of the liver in men: is presentation the same in men and women? Gut 2002;50(6):877–80.
31. Edmondson HA, Henderson B, Benton B. Liver-cell adenomas associated with use of oral contraceptives. N Engl J Med 1976;294(9):470–2.
32. Nault J-C, Bioulac-Sage P, Zucman-Rossi J. Hepatocellular benign tumors-from molecular classification to personalized clinical care. Gastroenterology 2013;144(5):888–902.
33. Belghiti J, Cauchy F, Paradis V, et al. Diagnosis and management of solid benign liver lesions. Nat Rev Gastroenterol Hepatol 2014;11(12):737–49.
34. Nault J-C, Couchy G, Balabaud C, et al. Molecular Classification of Hepatocellular Adenoma Associates With Risk Factors, Bleeding, and Malignant Transformation. Gastroenterology 2017;152(4):880–94.e6.
35. Chang CY, Hernandez-Prera JC, Roayaie S, et al. Changing epidemiology of hepatocellular adenoma in the United States: review of the literature. Int J Hepatol 2013;2013:604860.
36. Brunt EM, Sempoux C, Bioulac-Sage P. Hepatocellular adenomas: the expanding epidemiology. Histopathology 2021;79(1):20–2.
37. European Association for the Study of the Liver (EASL). EASL Clinical Practice Guidelines on the management of benign liver tumours. J Hepatol 2016;65(2):386–98.
38. Dokmak S, Paradis V, Vilgrain V, et al. A single-center surgical experience of 122 patients with single and multiple hepatocellular adenomas. Gastroenterology 2009;137(5):1698–705.
39. Farges O, Ferreira N, Dokmak S, et al. Changing trends in malignant transformation of hepatocellular adenoma. Gut 2011;60(1):85–9.
40. Védie A-L, Sutter O, Ziol M, et al. Molecular classification of hepatocellular adenomas: impact on clinical practice. Hepatic Oncol 2018;5(1). https://doi.org/10.2217/hep-2017-0023.
41. Julien C, Le-Bail B, Touhami KO, et al. Hepatocellular Adenoma Risk Factors of Hemorrhage: Size is not the only Concern! Single Center Retrospective Experience of 261 Patients. Ann Surg 2021. https://doi.org/10.1097/SLA.0000000000005108.
42. Beaufrère A, Paradis V. Hepatocellular adenomas: review of pathological and molecular features. Hum Pathol 2021;112:128–37.
43. Laumonier H, Bioulac-Sage P, Laurent C, et al. Hepatocellular adenomas: magnetic resonance imaging features as a function of molecular pathological classification. Hepatol Baltim Md 2008;48(3):808–18.
44. Ronot M, Bahrami S, Calderaro J, et al. Hepatocellular adenomas: accuracy of magnetic resonance imaging and liver biopsy in subtype classification. Hepatol Baltim Md 2011;53(4):1182–91.
45. Bise S, Frulio N, Hocquelet A, et al. New MRI features improve subtype classification of hepatocellular adenoma. Eur Radiol 2018. https://doi.org/10.1007/s00330-018-5784-5.
46. Nault J-C, Couchy G, Caruso S, et al. ASS1 and peri-portal gene expression in sonic hedgehog hepatocellular adenomas. Hepatol Baltim Md 2018. https://doi.org/10.1002/hep.29884.
47. Sala M, Gonzales D, Leste-Lasserre T, et al. ASS1 Overexpression: A Hallmark of Sonic Hedgehog Hepatocellular Adenomas; Recommendations for Clinical Practice. Hepatol Commun 2020;4(6):809–24.
48. Frulio N, Balabaud C, Laurent C, et al. Unclassified hepatocellular adenoma expressing ASS1 associated with inflammatory hepatocellular adenomas. Clin Res Hepatol Gastroenterol 2019. https://doi.org/10.1016/j.clinre.2019.03.012.
49. Gregory J, Paisant A, Paulatto L, et al. Limited added value of contrast-enhanced ultrasound over B-mode for the subtyping of hepatocellular adenomas. Eur J Radiol 2020;128:109027.
50. Grazioli L, Morana G, Kirchin MA, et al. Accurate differentiation of focal nodular hyperplasia from hepatic adenoma at gadobenate dimeglumine-enhanced MR imaging: prospective study. Radiology 2005;236(1):166–77.
51. Grazioli L, Bondioni MP, Haradome H, et al. Hepatocellular adenoma and focal nodular hyperplasia: value of gadoxetic acid-enhanced MR imaging in differential diagnosis. Radiology 2012;262(2):520–9.
52. Ba-Ssalamah A, Antunes C, Feier D, et al. Morphologic and Molecular Features of Hepatocellular Adenoma with Gadoxetic Acid-enhanced MR Imaging. Radiology 2015;277(1):104–13.
53. Agarwal S, Fuentes-Orrego JM, Arnason T, et al. Inflammatory hepatocellular adenomas can mimic focal nodular hyperplasia on gadoxetic acid-enhanced MRI. AJR Am J Roentgenol 2014;203(4):W408–14.
54. Thomeer MG, Willemssen FE, Biermann KK, et al. MRI features of inflammatory hepatocellular adenomas on hepatocyte phase imaging with liver-

specific contrast agents. J Magn Reson Imaging 2014;39(5):1259–64.
55. Tse JR, Naini BV, Lu DSK, et al. Qualitative and Quantitative Gadoxetic Acid-enhanced MR Imaging Helps Subtype Hepatocellular Adenomas. Radiology 2016;279(1):118–27.
56. Glockner JF, Lee CU, Mounajjed T. Inflammatory hepatic adenomas: Characterization with hepatobiliary MRI contrast agents. Magn Reson Imaging 2017;47:103–10.
57. Yoneda N, Matsui O, Kitao A, et al. Benign Hepatocellular Nodules: Hepatobiliary Phase of Gadoxetic Acid-enhanced MR Imaging Based on Molecular Background. Radiogr Rev Publ Radiol Soc N Am Inc 2016;36(7):2010–27.
58. Reizine E, Ronot M, Pigneur F, et al. Iso- or hyperintensity of hepatocellular adenomas on hepatobiliary phase does not always correspond to hepatospecific contrast-agent uptake: importance for tumor subtyping. Eur Radiol 2019. https://doi.org/10.1007/s00330-019-06150-7.
59. Reizine E, Ronot M, Ghosn M, et al. Hepatospecific MR contrast agent uptake on hepatobiliary phase can be used as a biomarker of marked β-catenin activation in hepatocellular adenoma. Eur Radiol 2021;31(5):3417–26.
60. Yoneda N, Matsui O, Kitao A, et al. Beta-catenin-activated hepatocellular adenoma showing hyperintensity on hepatobiliary-phase gadoxetic-enhanced magnetic resonance imaging and overexpression of OATP8. Jpn J Radiol 2012;30(9):777–82.
61. Rousseau C, Ronot M, Sibileau E, et al. Central element in liver masses, helpful, or pitfall? Abdom Imaging 2015;40(6):1904–25.
62. Vernuccio F, Gagliano DS, Cannella R, et al. Spectrum of liver lesions hyperintense on hepatobiliary phase: an approach by clinical setting. Insights Imaging 2021;12(1):8.
63. Young JR, Graham RP, Venkatesh SK, et al. 18F-FDG PET/CT of hepatocellular adenoma subtypes and review of literature. Abdom Radiol N Y 2021;46(6):2604–9.
64. Lim D, Lee SY, Lim KH, et al. Hepatic adenoma mimicking a metastatic lesion on computed tomography-positron emission tomography scan. World J Gastroenterol 2013;19(27):4432–6.
65. Barbier L, Nault J-C, Dujardin F, et al. Natural history of liver adenomatosis: a long-term observational study. J Hepatol 2019. https://doi.org/10.1016/j.jhep.2019.08.004.
66. Larssen TB, Rørvik J, Hoff SR, et al. The occurrence of asymptomatic and symptomatic simple hepatic cysts. A prospective, hospital-based study. Clin Radiol 2005;60(9):1026–9.
67. Tran Cao HS, Marcal LP, Mason MC, et al. Benign hepatic incidentalomas. Curr Probl Surg 2019;56(9):100642.
68. Lev-Toaff AS, Bach AM, Wechsler RJ, et al. The radiologic and pathologic spectrum of biliary hamartomas. AJR Am J Roentgenol 1995;165(2):309–13.
69. Borhani AA, Wiant A, Heller MT. Cystic hepatic lesions: a review and an algorithmic approach. AJR Am J Roentgenol 2014;203(6):1192–204.
70. Wilson JM, Groeschl R, George B, et al. Ciliated hepatic cyst leading to squamous cell carcinoma of the liver - A case report and review of the literature. Int J Surg Case Rep 2013;4(11):972–5.
71. Ziogas IA, van der Windt DJ, Wilson GC, et al. Surgical Management of Ciliated Hepatic Foregut Cyst. Hepatol Baltim Md 2020;71(1):386–8.
72. Kimura A, Makuuchi M, Takayasu K, et al. Ciliated hepatic foregut cyst with solid tumor appearance on CT. J Comput Assist Tomogr 1990;14(6):1016–8.
73. Shoenut JP, Semelka RC, Levi C, et al. Ciliated hepatic foregut cysts: US, CT, and contrast-enhanced MR imaging. Abdom Imaging 1994;19(2):150–2.
74. Kadoya M, Matsui O, Nakanuma Y, et al. Ciliated hepatic foregut cyst: radiologic features. Radiology 1990;175(2):475–7.
75. Fang S-H, Dong D-J, Zhang S-Z. Imaging features of ciliated hepatic foregut cyst. World J Gastroenterol 2005;11(27):4287–9.
76. Ansari-Gilani K, Modaresi Esfeh J. Ciliated hepatic foregut cyst: report of three cases and review of imaging features. Gastroenterol Rep 2017;5(1):75–8.
77. Rodriguez E, Soler R, Fernandez P. MR imagings of ciliated hepatic foregut cyst: an unusual cause of fluid-fluid level within a focal hepatic lesion (2005.4b). Eur Radiol 2005;15(7):1499–501.
78. Soares KC, Arnaoutakis DJ, Kamel I, et al. Cystic neoplasms of the liver: biliary cystadenoma and cystadenocarcinoma. J Am Coll Surg 2014;218(1):119–28.
79. Anderson MA, Dhami RS, Fadzen CM, et al. CT and MRI features differentiating mucinous cystic neoplasms of the liver from pathologically simple cysts. Clin Imaging 2021;76:46–52.
80. Kim JY, Kim SH, Eun HW, et al. Differentiation between biliary cystic neoplasms and simple cysts of the liver: accuracy of CT. AJR Am J Roentgenol 2010;195(5):1142–8.
81. Caseiro-Alves F, Brito J, Araujo AE, et al. Liver haemangioma: common and uncommon findings and how to improve the differential diagnosis. Eur Radiol 2007;17(6):1544–54.
82. Gore RM, Newmark GM, Thakrar KH, et al. Hepatic incidentalomas. Radiol Clin North Am 2011;49(2):291–322.
83. Harvey CJ, Albrecht T. Ultrasound of focal liver lesions. Eur Radiol 2001;11(9):1578–93.
84. Zarzour JG, Porter KK, Tchelepi H, et al. Contrast-enhanced ultrasound of benign liver lesions. Abdom Radiol N Y 2018;43(4):848–60.

85. Dietrich CF, Mertens JC, Braden B, et al. Contrast-enhanced ultrasound of histologically proven liver hemangiomas. Hepatol Baltim Md 2007;45(5):1139–45.
86. Duran R, Ronot M, Kerbaol A, et al. Hepatic hemangiomas: factors associated with T2 shine-through effect on diffusion-weighted MR sequences. Eur J Radiol 2014;83(3):468–78.
87. Vilgrain V, Boulos L, Vullierme MP, et al. Imaging of atypical hemangiomas of the liver with pathologic correlation. Radiogr Rev Publ Radiol Soc N Am Inc 2000;20(2):379–97.
88. Klotz T, Montoriol P-F, Da Ines D, et al. Hepatic haemangioma: common and uncommon imaging features. Diagn Interv Imaging 2013;94(9):849–59.
89. Byun JH, Kim TK, Lee CW, et al. Arterioportal shunt: prevalence in small hemangiomas versus that in hepatocellular carcinomas 3 cm or smaller at two-phase helical CT. Radiology 2004;232(2):354–60.
90. Di Carlo I, Koshy R, Al Mudares S, et al. Giant cavernous liver hemangiomas: is it the time to change the size categories? Hepatobiliary Pancreat Dis Int 2016;15(1):21–9.
91. Makhlouf HR, Ishak KG. Sclerosed hemangioma and sclerosing cavernous hemangioma of the liver: a comparative clinicopathologic and immunohistochemical study with emphasis on the role of mast cells in their histogenesis. Liver 2002;22(1):70–8.
92. Jia C, Liu G, Wang X, et al. Hepatic sclerosed hemangioma and sclerosing cavernous hemangioma: a radiological study. Jpn J Radiol 2021. https://doi.org/10.1007/s11604-021-01139-z.
93. Kim Y-Y, Kang TW, Cha DI, et al. Gadoxetic acid-enhanced MRI for differentiating hepatic sclerosing hemangioma from malignant tumor. Eur J Radiol 2021;135:109474.
94. Stoupis C, Taylor HM, Paley MR, et al. The Rocky liver: radiologic-pathologic correlation of calcified hepatic masses. Radiogr Rev Publ Radiol Soc N Am Inc 1998;18(3):675–85 [quiz: 726].
95. Goodman ZD, Ishak KG. Angiomyolipomas of the liver. Am J Surg Pathol 1984;8(10):745–50.
96. Tsui WM, Colombari R, Portmann BC, et al. Hepatic angiomyolipoma: a clinicopathologic study of 30 cases and delineation of unusual morphologic variants. Am J Surg Pathol 1999;23(1):34–48.
97. Lee SJ, Kim SY, Kim KW, et al. Hepatic Angiomyolipoma Versus Hepatocellular Carcinoma in the Noncirrhotic Liver on Gadoxetic Acid-Enhanced MRI: A Diagnostic Challenge. AJR Am J Roentgenol 2016;207(3):562–70.
98. Black ME, Hedgire SS, Camposano S, et al. Hepatic manifestations of tuberous sclerosis complex: a genotypic and phenotypic analysis. Clin Genet 2012;82(6):552–7.
99. Prasad SR, Wang H, Rosas H, et al. Fat-containing lesions of the liver: radiologic-pathologic correlation. Radiogr Rev Publ Radiol Soc N Am Inc 2005;25(2):321–31.
100. Ji J, Lu C, Wang Z, et al. Epithelioid angiomyolipoma of the liver: CT and MRI features. Abdom Imaging 2013;38(2):309–14.
101. O'Malley ME, Chawla TP, Lavelle LP, et al. Primary perivascular epithelioid cell tumors of the liver: CT/MRI findings and clinical outcomes. Abdom Radiol N Y 2017;42(6):1705–12.
102. Huang Z, Wu X, Li S, et al. Contrast-Enhanced Ultrasound Findings and Differential Diagnosis of Hepatic Epithelioid Angiomyolipoma Compared with Hepatocellular Carcinoma. Ultrasound Med Biol 2020;46(6):1403–11.
103. Balci NC, Tunaci A, Akinci A, et al. Granulomatous hepatitis: MRI findings. Magn Reson Imaging 2001;19(8):1107–11.
104. Mortelé KJ, Segatto E, Ros PR. The infected liver: radiologic-pathologic correlation. Radiogr Rev Publ Radiol Soc N Am Inc 2004;24(4):937–55.
105. Harrington PT, Gutiérrez JJ, Ramirez-Ronda CH, et al. Granulomatous hepatitis. Rev Infect Dis 1982;4(3):638–55.
106. Drebber U, Kasper H-U, Ratering J, et al. Hepatic granulomas: histological and molecular pathological approach to differential diagnosis–a study of 442 cases. Liver Int 2008;28(6):828–34.
107. Lee NK, Kim S, Kim DU, et al. Diffusion-weighted magnetic resonance imaging for non-neoplastic conditions in the hepatobiliary and pancreatic regions: pearls and potential pitfalls in imaging interpretation. Abdom Imaging 2015;40(3):643–62.
108. Zhang L, Lin WM, Li H, et al. Hepatic nontuberculous mycobacterial granulomas in patients with cancer mimicking metastases: an analysis of three cases. Quant Imaging Med Surg 2019;9(6):1126–31.
109. Pack GT, Baker HW. Total right hepatic lobectomy; report of a case. Ann Surg 1953;138(2):253–8.
110. Yamamoto H, Yamaguchi H, Aishima S, et al. Inflammatory myofibroblastic tumor versus IgG4-related sclerosing disease and inflammatory pseudotumor: a comparative clinicopathologic study. Am J Surg Pathol 2009;33(9):1330–40.
111. Zen Y, Fujii T, Sato Y, et al. Pathological classification of hepatic inflammatory pseudotumor with respect to IgG4-related disease. Mod Pathol 2007;20(8):884–94.
112. Park JY, Choi MS, Lim Y-S, et al. Clinical features, image findings, and prognosis of inflammatory

pseudotumor of the liver: a multicenter experience of 45 cases. Gut Liver 2014;8(1):58–63.

113. Someren A. Inflammatory pseudotumor" of liver with occlusive phlebitis: report of a case in a child and review of the literature. Am J Clin Pathol 1978; 69(2):176–81.

114. Lee SL, DuBois JJ. Hepatic inflammatory pseudotumor: case report, review of the literature, and a proposal for morphologic classification. Pediatr Surg Int 2001;17(7):555–9.

115. Nam KJ, Kang HK, Lim JH. Inflammatory pseudotumor of the liver: CT and sonographic findings. AJR Am J Roentgenol 1996;167(2):485–7.

116. Kong W-T, Wang W-P, Cai H, et al. The analysis of enhancement pattern of hepatic inflammatory pseudotumor on contrast-enhanced ultrasound. Abdom Imaging 2014;39(1):168–74.

117. Patnana M, Sevrukov AB, Elsayes KM, et al. Inflammatory pseudotumor: the great mimicker. AJR Am J Roentgenol 2012;198(3):W217–27.

118. Ichikawa S, Motosugi U, Suzuki T, et al. Imaging features of hepatic inflammatory pseudotumor: distinction from colorectal liver metastasis using gadoxetate disodium-enhanced magnetic resonance imaging. Abdom Radiol N Y 2020;45(8): 2400–8.

119. Chang AI, Kim YK, Min JH, et al. Differentiation between inflammatory myofibroblastic tumor and cholangiocarcinoma manifesting as target appearance on gadoxetic acid-enhanced MRI. Abdom Radiol N Y 2019;44(4):1395–406.